Supporting Information

# Primer extension activating 3D DNAzyme walker for telomerase activity in situ imaging and sensitive detection

Xiaoting Liu [a,b], Liyan Zhang [b], Ling Lu [a], Wei Jiang [b], and Nan Zhang*[,a]

[a] Research Center of Basic Medicine, Breast Center, Jinan Central Hospital, Cheeloo College of Medicine, Shandong University, Jinan 250013, P. R. China.

[b] School of Chemistry and Chemical Engineering, Shandong University, Jinan 250100, P. R. China.

Corresponding author:

**Nan Zhang***[,a]: E-mail: zlkzn2016@126.com.

**Table S1**: Sequences of oligonucleotides used in this study

| Name | Sequences (5'-3') |
|---|---|
| Telomerase primer | AATCCGTCGAGCAGAGTT |
| DNAzyme hairpin | (Cy5)-TGATGTTGATCCGAGCCGGTCGAAAGGGTTAGGGTTTTTTTTTTTTTTTTTTTTTTTTTTTCCCTAACCCTAACTCTGCTCGACGGATT-SH |
| Track strand | SH-TTTTTTTTTTTTTTCGACGGTTTTTCCTAACCCTrAGTCAACATCATTTTTCCGTCG-FAM |

Note: The green part of the DNAzyme hairpin is the complementary sequence of the telomerase primer, and the blue part represents the 8-17 DNAzyme sequence; the red rA in the substrate hairpin represents adenine ribonucleotides.

**Table S2**: Sequences of qRT-PCR primer in this study

| Name | Sequences (5'-3') |
|---|---|
| TERT forward | GGAAGAGTGTCTGGAGCAAGTT |
| TERT reverse | TGGGGATGAAGCGGAGTC |
| GAPDH forward | TGGGTGTGAACCATGAGAAGT |
| GAPDH reverse | TGAGTCCTTCCACGATACCAA |

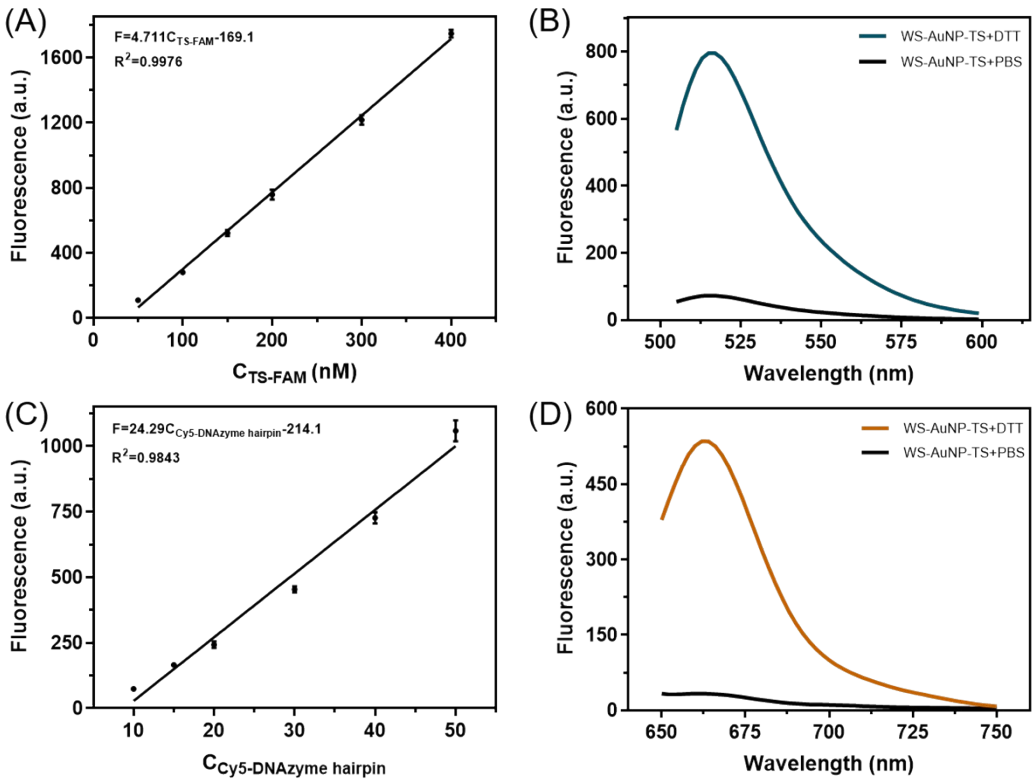


**Figure S1** (A) The standard curve of FAM-labeled track strand, the linear equation is $F = 4.711C_{TS-FAM} - 169.1$, $R^2 = 0.9976$; (B) Fluorescence spectra of WS-AuNP-TS (5.0 nM) after incubation with PBS and DTT (20 mM), respectively, FAM-labeled track strand was recorded with 488 nm excitation wavelength; (C) The standard curve of Cy5-labeled DNAzyme hairpin, the linear equation is $F = 24.29C_{Cy5\text{-}DNAzyme\ hairpin} - 214.1$, $R^2 = 0.9843$; (D) Fluorescence spectra of WS-AuNP-TS (5.0 nM) after incubation with PBS and DTT (20 mM), respectively, Cy5-labeled DNAzyme hairpin was recorded with 632 nm excitation wavelength.

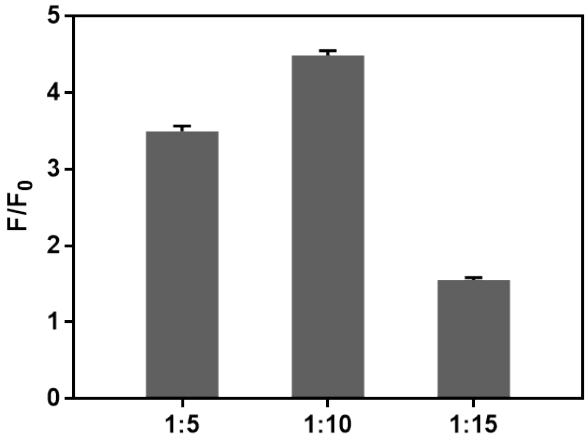


**Figure S2** The effect of the modification ratio of walking strand and track strand on $F/F_0$.

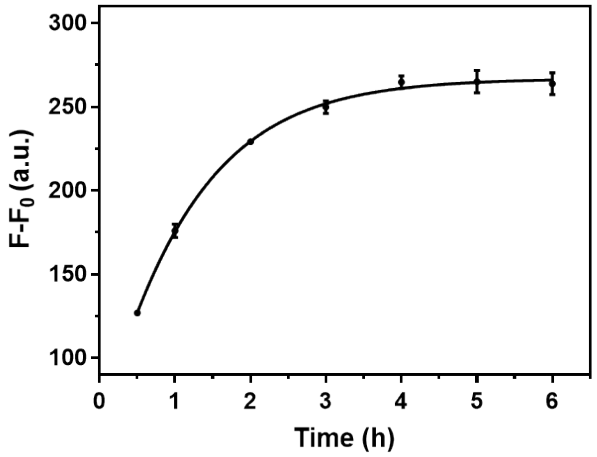


**Figure S3** The effect of reaction time on the net signal of the system.

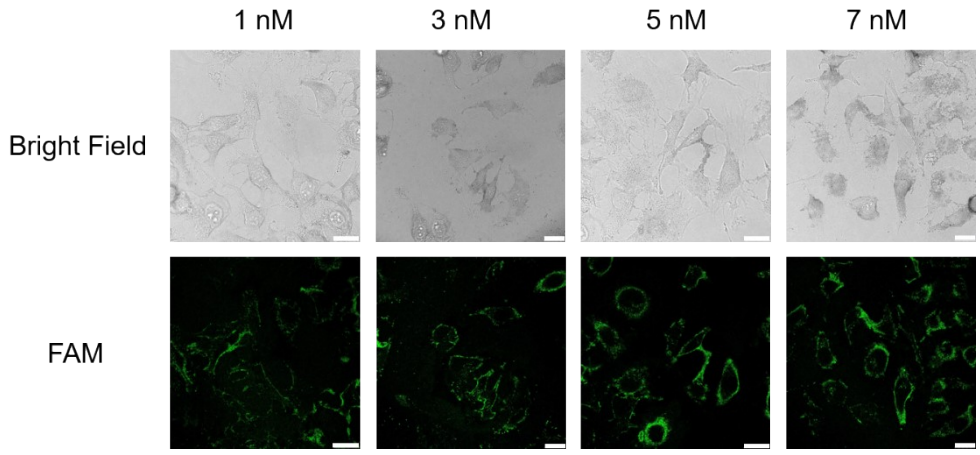


**Figure S4** Selection of WS-AuNP-TS concentration. Scale bar: 25 μm.

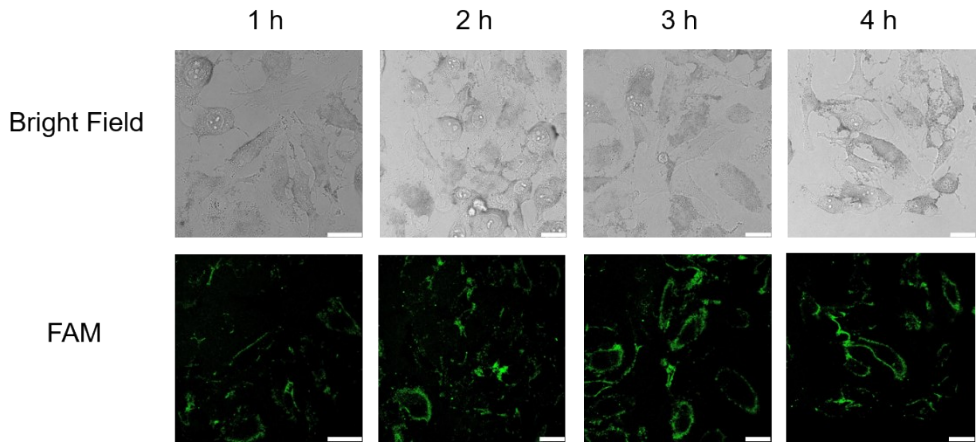


**Figure S5** Selection of WS-AuNP-TS incubation time. Scale bar: 25 μm.

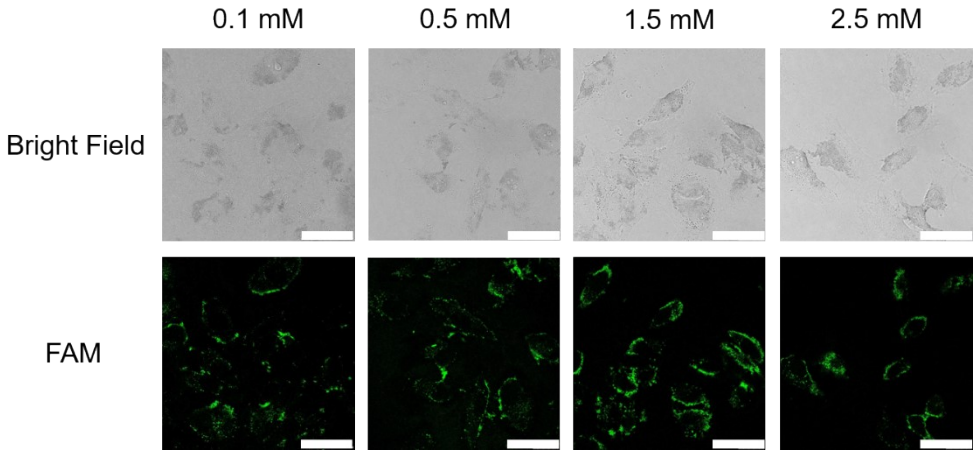


**Figure S6** Selection of $Mn^{2+}$ concentration. Scale bar: 50 μm.

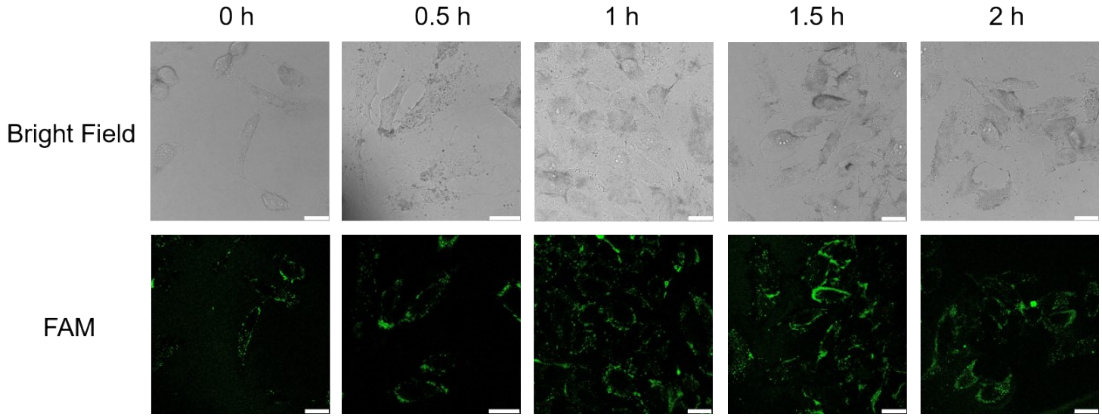


**Figure S7** Selection of $Mn^{2+}$ incubation time. Scale bar: 25 μm.

**Table S3:** Comparison of the detection performance for telomerase activity with some reported works.

| Strategy | Detection mode | LOD | Reference |
|---|---|---|---|
| ECL sensor using G-quadruplex and luminol modified AuNPs | ECL | 148 cells | [1] |
| Telomere complementary oligonucleotide functionalized AuNPs probe | UV-vis | 100 cells | [2] |
| Label-free colorimetry based on conjugate hemin-graphene | UV-vis | 60 cells/mL | [3] |
| Ratiometric sensing based on structure-switching DNA | FRET | 33 cells | [4] |
| Enzyme-free signal amplification-HCR | Fluorescence | 480 cells | [5] |
| Single quantum dot-based biosensor | Fluorescence | 185 cells | [6] |
| Tetrahedral DNA nanoprobe | Fluorescence | 35 cells | [7] |
| Fluorescent tungsten oxide quantum dots | Fluorescence | 17 cells | [8] |
| Controllable aggregation of quantum dots | Fluorescence | 13 cells | [9] |
| Primer extension activated 3D DNAzyme walker | Fluorescence | 10 cells | This work |

## Reference

[1] H.R. Zhang, Y.Z. Wang, M.S. Wu, Q.M. Feng, H.W. Shi, H.Y. Chen, J.J. Xu, Visual electrochemiluminescence detection of telomerase activity based on multifunctional Au nanoparticles modified with G-quadruplex deoxyribozyme and luminol, Chem Commun 50 (2014) 12575-12577. 10.1039/c4cc06302c

[2] J.S. Wang, L. Wu, J.S. Ren, X.G. Qu, Visual detection of telomerase activity with a tunable dynamic range by using a gold nanoparticle probe-based hybridization protection strategy, Nanoscale 6 (2014) 1661-1666. 10.1039/c3nr05185d

[3] X.L. Xu, M. Wei, Y.J. Liu, X. Liu, W. Wei, Y.J. Zhang, S.Q. Liu, A simple, fast, label-free colorimetric method for detection of telomerase activity in urine by using hemin-graphene conjugates, Biosens Bioelectron 87 (2017) 600-606. 10.1016/j.bios.2016.09.005

[4] X.J. Yang, K. Zhang, T.T. Zhang, J.J. Xu, H.Y. Chen, Reliable forster resonance energy transfer probe based on structure-switching DNA for ratiometric sensing of telomerase in living cells, Anal Chem 89 (2017) 4216-4222. 10.1021/acs.analchem.7b00267

[5] M. Hong, L.D. Xu, Q.W. Xue, L. Li, B. Tang, Fluorescence imaging of intracellular telomerase activity using enzyme-free signal amplification, Anal Chem 88 (2016) 12177-12182. 10.1021/acs.analchem.6b03108

[6] Z. Yi, H.B. Wang, K. Chen, Q. Gao, H. Tang, R.Q. Yu, X. Chu, A novel electrochemical biosensor for sensitive detection of telomerase activity based on structure-switching DNA, Biosens Bioelectron 53 (2014) 310-315. 10.1016/j.bios.2013.09.072

[7] X.M. Yue, Y.Q. Qiao, D.N. Gu, Z.X. Wu, W.H. Zhao, X.Y. Li, Y.M. Yin, W. Zhao, D.M. Kong, R.M. Xi, M. Meng, Reliable FRET-ON imaging of telomerase in living cells by a tetrahedral DNA nanoprobe integrated with structure-switchable molecular beacon, Sensor Actuat B-Chem 312 (2020) 127943. 10.1016/j.snb.2020.127943

[8] L. Zhang, J.Q. Chen, M.F. Hong, R.P. Liang, J.D. Qiu, Facile synthesis of fluorescent tungsten oxide quantum dots for telomerase detection based on the inner filter effect, Analyst 145(2020) 2570-2579. 10.1039/D0AN00296H

[9] L. Zhang, M.F. Hong, J. Peng, J.Q. Chen, R.P. Liang, J.D. Qiu, A sensitive assay of telomerase activity based on the controllable aggregation of quantum dots, Sensor Actuat B-Chem 277 (2018) 22-29. 10.1016/j.snb.2018.08.107